ORGANIC LETTERS

2013
Vol. 15, No. 16
4058–4061

Bimodal Calix[2]triazole[2]arene Fluorescent Ionophore

Jihee Cho,[†] Tuhin Pradhan,[‡] Jong Seung Kim,*[,‡] and Sanghee Kim*[,†]

College of Pharmacy, Seoul National University, Seoul 151-742, Korea, and Department of Chemistry, Korea University, Seoul 136-701, Korea

jongskim@korea.ac.kr; pennkim@snu.ac.kr

Received May 24, 2013

ABSTRACT

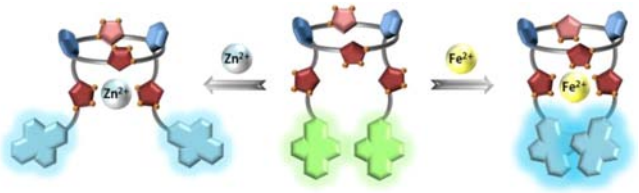

Pyrene-appended calix[2]triazole[2]arene capable of bimodal sensing has been synthesized. Upon addition of Zn^{2+} (or Cd^{2+}), it selectively exhibits an enhanced monomeric emission (~13−20-fold) over other metal ions. On the other hand, it displays excellent selectivity for Fe^{2+} over other metal ions (even over Fe^{3+}) from the angle of excimeric emissions (10-fold enhancement). Density Functional Theory (DFT) based theoretical calculations distinguished the bimodal activity of the probe and supported the experimental observations.

Due to the distinct three-dimensional shapes, calixarenes have received considerable attention in various fields, especially in molecular recognition.[1] Recently, increasing attention has also been focused on the heterocalixarenes in which phenol units of calixarene are replaced by aromatic heterocycles.[2] In this regard, we have recently reported the design and synthesis of calix[2]triazole[2]arene (**1**, Scheme 1) as a new class of hybrid heterocalixarene.[3] We hypothesized that the inherent physicochemical properties of 1,2,3-triazole[4] would alter the electronic environment around the calixarene annulus and induce unique cavity structures, thereby causing changes in its interactions with other molecules and ions.

In the present manuscript, we report a newly synthesized pyrenyl-appended calix[2]triazole[2]arene **2** which functions as a bimodal fluorescent ionophore toward the Zn^{2+} (or Cd^{2+}) ion and Fe^{2+}. Compound **2** shows its conformational changes upon metal ion encapsulation to give excimeric emission changes of two pyrenes, which is well supported by DFT calculations.

The synthesis began with the reaction of **1** with propargyl bromide (15 equiv) in the presence of NaH in DMF at −40 °C to give **3** in a quantitative yield. The intermolecular copper(I)-catalyzed azide−alkyne cycloaddition (CuAAC) reaction[5] of alkyne **3** with azidopyrene **4**[6] provided desired product **2** in 96% yield.

The fluorescence spectra of **2** exhibits a weak monomer emission at 378 and 397 nm and a strong excimer emission at 476 nm (Figure 1a) arising from the intramolecular π-stacked pyrene units, which is typically seen in bipyrene containing molecules.[7] The ^1H NMR spectrum of **2** in CD_3CN at rt indicated it is in a C_2 symmetry. Aromatic

[†] Seoul National University.
[‡] Korea University.

(1) For comprehensive reviews on calixarenes, see: (a) Asfari, Z.; Bőhmer, V.; Harrowfield, J.; Vicens, J. *Calixarenes 2001*; Kluwer: Dordrecht, 2001. (b) Mandolini, L.; Ungaro, R. *Calixarenes in Action*; Imperial College Press: London, 2000. (c) Gutsche, C. D. *Calixarenes: An introduction (Monographs in Supramolecular Chemistry)*, 2nd ed.; The Royal Society of Chemistry: Cambridge, 2008.

(2) For reviews on heterocalixarenes, see: (a) Kumar, S.; Paul, D.; Singh, H. In *Advances in Heterocyclic Chemistry*; Katritzky, A. R., Ed.; Elsevier: Amsterdam, 2005; Vol. 89, p 65. (b) Sliwa, W. *Chem. Heterocycl. Compd.* **2004**, *40*, 683.

(3) Cho, J.; Lee, S.; Hwang, S.; Kim, S. H.; Kim, J. S.; Kim, S. *Eur. J. Org. Chem.* **2013**, 4614.

(4) For reviews on 1,2,3-triazoles, see:(a) Juríček, M.; Kouwer, P. H. J.; Rowan, A. E. *Chem. Commun.* **2011**, *47*, 8740. (b) Bock, V. D.; Hiemstra, H.; van Maarseveen, J. H. *Eur. J. Org. Chem.* **2006**, 51.

(5) (a) Rostovtsev, V. V.; Green, L. G.; Fokin, V. V.; Sharpless, K. B. *Angew. Chem., Int. Ed.* **2002**, *41*, 2596. (b) Tornøe, C. W.; Christensen, C.; Meldal, M. *J. Org. Chem.* **2002**, *67*, 3057.

(6) Park, S. Y.; Yoon, J. H.; Hong, C. S.; Souane, R.; Kim, J. S.; Matthews, S. E.; Vicens, J. *J. Org. Chem.* **2008**, *73*, 8212.

(7) (a) Broan, C. J. *Chem. Commun.* **1996**, 699. (b) Kim, H. J.; Lee, M. H.; Mutihac, L.; Vicens, J.; Kim, J. S. *Chem. Soc. Rev.* **2012**, *41*, 1173. (c) Kim, J. S.; Quang, D. T. *Chem. Rev.* **2007**, *107*, 3780. (d) Quang, D. T.; Kim, J. S. *Chem. Rev.* **2010**, *110*, 6280.

10.1021/ol401469z
Published on Web 08/05/2013

Scheme 1. Synthesis of Pyrenyl-Appended Calix[2]triazole[2]-arene **2** and Structure of Pyrenyl-Appended Calix[4]arene **5**

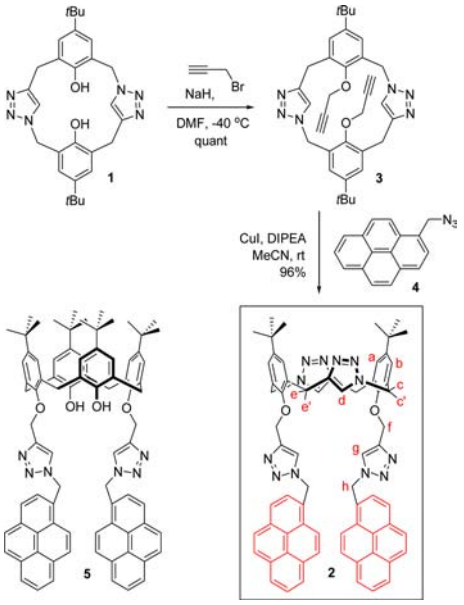

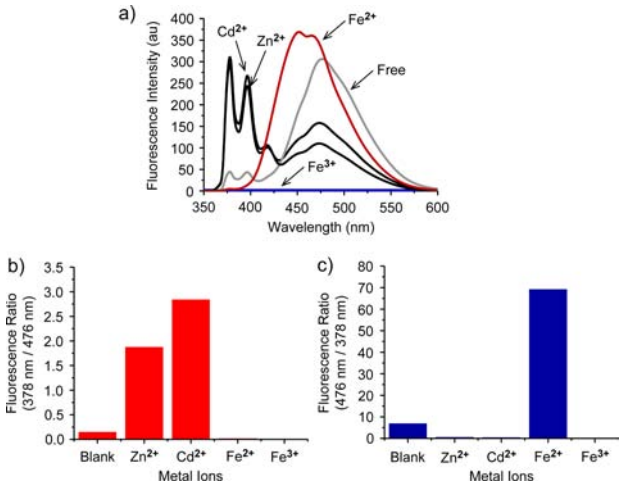

Figure 1. (a) Fluorescence spectra of **2** (6 μM) in acetonitrile in the presence of 40 equiv of Zn^{2+}, Cd^{2+}, Fe^{2+}, or Fe^{3+} (excitation at 342 nm). (b) Fluorescence ratio (F_{378}/F_{476}) histogram of **2** (6 μM) with 40 equiv of Zn^{2+}, Cd^{2+}, Fe^{2+}, or Fe^{3+}. (c) Fluorescence ratio (F_{476}/F_{378}) histogram of **2** (6 μM) with 40 equiv of Zn^{2+}, Cd^{2+}, Fe^{2+}, or Fe^{3+}.

protons (H_a and H_b) in phenyl rings and triazole protons (H_d) in the annulus show a NOESY cross-peak with a different methylene proton (H_c, H_e vs $H_{c'}$, $H_{e'}$) as seen in Figure S11. The other NOESY correlation between triazole protons (H_d) in the annulus and methylene protons (H_f) of the OCH_2-triazole linker was also observed (Figure S11). Both fluorescence and NMR experimental results led us to conclude that probe **2** is in such a conformation where the phenolic oxygen atoms and triazole protons (H_d) are on the same side of the annulus as depicted in Scheme 1.

To gain insight into the metal ion binding properties, fluorescence changes of **2** were examined upon the addition of perchlorate salts of various metal cations (40 equiv) (Figures 1a and S2). Unlike other metal ions, in the presence of a Zn^{2+} or Cd^{2+} ion, probe **2** showed a ratiometric change in such a manner that monomer emission markedly enhanced (~13−20-fold compared to free ligand) and excimer emission dramatically declined, selectively over other metal ions (Figure 1b). The metal binding properties of **2** in regard to monomer and excimer changes are similar to those of conventional calix[4]arene sensor **5** (Scheme 1) previously reported by us for selective recognition of Cd^{2+} and Zn^{2+} over a wide range of metal cations.[6]

More interesingly, a significant difference in fluorescence changes of **2** from **5** was observed upon addition of Fe^{2+}. Addition of Fe^{2+} to a solution of **5** gave quenched emission in both monomer and excimer emissions (Figure S5), whereas probe **2** gave enhanced fluorescence as well as a blue shift of the excimer emission from 476 to 452 nm (Figure 1a). This type of emission refers to a static pyrene excimer. The shift from a dynamic to a static excimer upon the addition of Fe^{2+} was evident in the excitation spectra (Figure S4). It should be noteworthy that **2** can even distinguish Fe^{2+} from Fe^{3+} with respect to the excimeric emission changes, which has been rarely reported so far.[8,9] In competition experiments, when various metal ions (40 equiv) were added to a solution of the **2**−Fe^{2+} complex, no excimer emission shift was observed, confirming that probe **2** functions as a Fe^{2+}-specific fluorescent probe even in the presence of many different metal ions as well (Figure S6). Herein we verify once again that probe **2** exhibits excellent selectivity for Fe^{2+} over other metal ions from the angle of excimeric emissions (10-fold increase) as seen in Figure 1c. Therefore, as the monomeric and excimeric emission have a large band separation (378 and 476 nm, respectively), probe **2** can distinctly identify Zn^{2+} (or Cd^{2+}) and Fe^{2+} with respect to its monomeric and excimeric emission changes in a qualitative and quantitative manner.

The ^{1}H NMR binding study was undertaken to determine the complexation mode of **2** toward metal ions. In the presence of Zn^{2+} or Cd^{2+}, the proton resonances of H_g shifted downfield, and the methylene protons H_f exhibited upfield shifts (Figure 2c). These chemical shift changes reflect the triazole rings in the appendage are involved in the metal ion binding.[6] The NOESY correlation of H_d with H_f as well as the methylene protons proximal to the phenolic oxygen atoms ($H_{c'}$ and $H_{e'}$) were observed in the spectrum of **2**−Cd^{2+} (Figure S13). This observation implies that H_d and H_g are on the same side of the annulus,

(8) (a) Pathak, R. K.; Dessingou, J.; Hinge, V. K.; Thawari, A. G.; Basu, S. K.; Rao, C. P. *Anal. Chem.* **2013**, *85*, 3707. (b) Wei, Y.; Aydin, Z.; Zhang, Y.; Liu, Z.; Guo, M. *ChemBioChem* **2012**, *13*, 1569. (c) Sen, S.; Sarkar, S.; Chattopadhyay, B.; Moirangthem, A.; Basu, A.; Dhara, K.; Chattopadhyay, P. *Analyst* **2012**, *137*, 3335. (d) Bhaumik, C.; Das, S.; Maity, D.; Baitalik, S. *Dalton Trans.* **2011**, *40*, 11795.

(9) (a) Li, P.; Fang, L.; Zhou, H.; Zhang, W.; Wang, X.; Li, N.; Zhong, H.; Tang, B. *Chem.—Eur. J.* **2011**, *17*, 10520. (b) Kumar, M.; Kumar, N.; Bhalla, V. *Tetrahedron Lett.* **2011**, *52*, 4333. (c) Fan, L.-J.; Jones, W. E., Jr. *J. Am. Chem. Soc.* **2006**, *128*, 6784.

and thereby the shielding effects of aromatic rings causing upfield shift of H_d could be excluded. As a result, similar to the proposed binding mode in **5** for cations, the Zn^{2+} and Cd^{2+} ions may bind to the nitrogens of the appended triazole units in **2**, but not to those of the annulus triazole units (Figure 2a).

In the presence of Fe^{2+}, we observed that the H_g broadened and shifted downfield as seen in Figure 2d.[10] In addition, the triazole protons in the annulus (H_d) also shifted downfield with peak broadening. These spectral shifts suggest that, upon addition of Fe^{2+} ion, conformational changes of the calix-annulus occur to adopt the Fe^{2+} ions (Figure 2b).

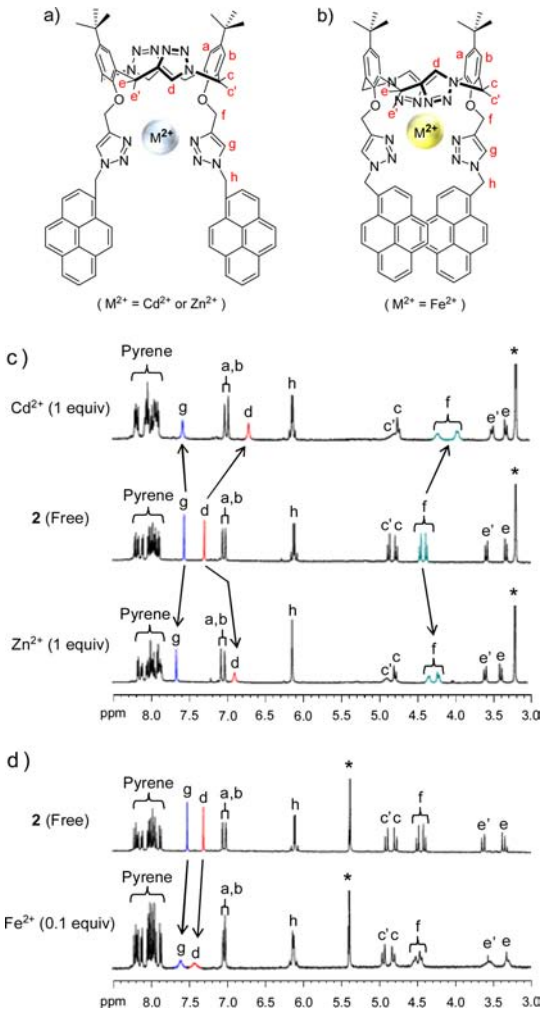

Figure 2. Proposed structures of **2** in the presence of (a) Cd^{2+} or Zn^{2+} and (b) Fe^{2+}. ^1H NMR spectrum of **2** (c) in CD_3CN/CD_3OD (9:1, v/v) and with $Cd(ClO_4)_2$ (1 equiv) or $Zn(ClO_4)_2$ (1 equiv), where * denotes the residual proton signals from CD_3OD, with protons labeled as in Figure 2a, and (d) in CD_3CN/CD_2Cl_2 (7:1, v/v) and with $Fe(ClO_4)_2$ (0.1 equiv), where * denotes the residual proton signals from CD_2Cl_2, with protons labeled as in Figure 2b.

To attain deeper insight into the origin of experimentally observed fluorescence changes, we carried out density functional theory (DFT) based theoretical calculations. We have chosen Zn^{2+} and Fe^{2+} as metal ions for the model calculations. The optimized structure of **2** and the **2**–Zn^{2+} and **2**–Fe^{2+} complexes have been shown in Figure 3. We have defined three parameters theoretically for the qualitative evaluation of intramolecular excimer formation between two pyrenes of **2**, **2**–Zn^{2+}, and **2**–Fe^{2+}. The parameters are as follows: (1) Dihedral angle (DHA): dihedral angle among the carbons C_1, C_2, C_3, and C_4 (as shown in Figures 3 and S1 by blue dotted lines) can be the measure of parallelism between the two pyrenes. As the DHA decreases, the parallelism increases. The DHA for **2**, **2**–Zn^{2+}, and **2**–Fe^{2+} are respectively −19.6°, −65.3°, and 7.9° (Table 1), which indicates that two pyrenes are nearly perpendicular to each other in **2**–Zn^{2+} and nearly parallel to each other in **2**–Fe^{2+}. The parallelism is much better in **2** than in **2**–Zn^{2+} explaining partially the better excimer formation in **2** than in **2**–Zn^{2+}. The parallel arrangement between two pyrenes is a criterion for excimer formation.[11] (2) Vertical displacement (Δ; Å): vertical displacement is the vertical length between the two lines passing through the carbons C_1 and C_4 (as shown in Figure 3b). The minimum vertical displacement ensures the maximum overlap integral between two parallel pyrenes. The vertical displacement is the least in **2**–Fe^{2+} and the highest in **2**–Zn^{2+} (Table 1). (3) Minimum distance (D): this is the closest separation between the two pyrenes (Figure S1). It is found that excimer formation between two pyrenes is favorable when the smallest distance between their molecular centers ranges from ∼4 to 10 Å.[11] The minimum distances for all the systems (**2**, **2**–Zn^{2+}, and **2**–Fe^{2+}) are in the range of excimer formation (4.1–4.6 Å, Table 1). By considering the above three parameters for all the systems (Table 1), we observed that the **2**–Fe^{2+} system possessed the chance of maximum overlapping between two pyrenes and **2**–Zn^{2+} possessed the minimum for intramolecular excimer formation, which validated the experimental observations.

Fe^{2+} binds **2** more strongly than Zn^{2+} (binding energies are respectively −382.9 and −359.4 kcal/mol in gas phase). The binding mode of Fe^{2+} with **2** also differs from Zn^{2+} (Figure 3). Two triazole rings from the appendage in the **2**–Zn^{2+} system participate in binding, whereas one triazole ring from the appendage and another from the annulus in the **2**–Fe^{2+} system participate in binding. The different binding mode and stronger binding in the **2**–Fe^{2+} system may lead to the highest overlapping between two pyrene planes for the excimer formation. To verify this, we removed the metal ions from **2**–Zn^{2+} and **2**–Fe^{2+} and repeated the optimization for the metal-free systems without perturbing any other geometrical parameters. We found that for all the cases removing metal ions induced significant changes in the theoretical parameters (Table 1 and Figure S1). For example, DHA changes from 7.9° to −25.5° and the minimum distance (D) changes from

(10) In the presence of 1 equiv of Fe^{2+}, the complexation mode could not be satisfactorily determined because the paramagnetic nature of Fe^{2+} leads to severe peak broadening. Some informative changes were observed only with the addition of subequivalent amounts of Fe^{2+}.

(11) Winnik, F. M. *Chem. Rev.* **1993**, *93*, 587.

4.1 to 8.3 Å in the case of **2**−Fe^{2+}. This supports the notion that the different binding mode and binding strength are the driving forces for the experimentally observed differences in excimer−monomer formation upon addition of various metal ions.

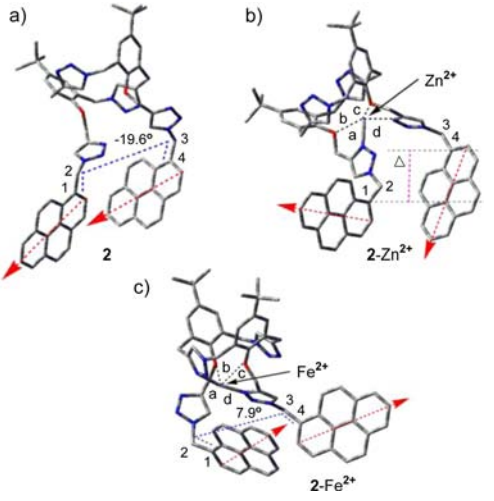

Figure 3. Optimized structures of (a) **2**, (b) **2**−Zn^{2+} complex, and (c) **2**−Fe^{2+} complex. Structures were optimized at the B3LYP/6-31G(d) level of theory. H-atoms are removed for clarity. Black dotted lines indicate the bond distances (a, b, c, and d) between metal ions (b) Zn^{2+} and (c) Fe^{2+} with **2**. Bond distances (a, b, c, and d) in (b) are respectively 2.02, 2.38, 2.13, and 2.08 Å. Bond distances (a, b, c, and d) in (c) are respectively 1.92, 2.02, 2.95, and 1.94 Å. Pink dotted line represents the vertical displacement (Δ) between two pyrene planes. Red arrows indicate the directions of the planes containing pyrenes. Blue dotted lines indicate the dihedral angle (DHA) among the carbons numbered as 1, 2, 3, and 4.

In summary, pyrene-appended calix[2]triazole[2]arene **2** was newly synthesized and its conformations were investigated by NMR and DFT calculations. We found that probe **2** functions in bimodal fluorescent sensing. Upon addition of Zn^{2+} (or Cd^{2+}), it displays an enhanced monomeric emission (∼13−20-fold compared to free ligand) selectively over other metal ions. On the other hand, it exhibits excellent selectivity for Fe^{2+} over other metal ions (even over Fe^{3+} ion) from the angle of excimeric emissions (10-fold increase) by the conformational change of the calix annulus. As the monomeric and excimeric emission have a large band separation (378 and 476 nm, respectively), the probe can distinctly identify Zn^{2+} (or Cd^{2+}) and Fe^{2+} in a qualitative and quantitative manner. Density Functional Theory (DFT) based theoretical calculations distinguished the bimodal activity of the probe and supported the experimental observations. This study provided insight into the distinctive properties of calix[2]-triazole[2]arenes over conventional calix[4]arenes.

Table 1. Calculated Parameters which Estimate the Parallelism and Overlapping between Two Pyrenes in **2** and Complexes[a]

	compd with Zn^{2+}			compd with Fe^{2+}	
parameters	with Zn^{2+}	after removing Zn^{2+}	compd	with Fe^{2+}	after removing Fe^{2+}
dihedral angle (DHA)	−65.3°	74.5°	−19.6°	7.9°	−25.5°
vertical displacement (Δ; Å)	4.2	4.2	2.8	1.5	2.5
min. distance (D; Å)	4.6	12.2	4.3	4.1	8.3

[a] Structures were optimized at the B3LYP/6-31G(d) level of theory. Carbons 1, 2, 3, and 4 (Figures 3 and S1) constitute the dihedral angle (DHA), which defines the state of parallel between two pyrenes of **2** and its complexes. Vertical displacement (Δ) between two pyrenes is the minimum distance between the two lines passing through the carbons 1 and 4 (as shown in Figure 3). Minimum distance (D) is the closest distance between two pyrenes as shown in Figure S1.

Acknowledgment. This research was supported by the Basic Science Research Program through the National Research Foundation of Korea (Nos. 2012-0001802 and 2012-0000243).

Supporting Information Available. Experimental procedure, characterization data, computational details, and additional spectra (UV/vis absorption, fluorescence, NMR). This material is available free of charge via the Internet at http://pubs.acs.org.

The authors declare no competing financial interest.